A Study on Optimization of Albedo Boundary Conditions for the Deterministic Truncation of Monte Carlo Solutions

Inhyung Kim[a], Yonghee Kim [a*]
[a] Nuclear and Quantum Engineering, Korea Advanced Institute of Science and Technology (KAIST),
291 Daehak-ro, Yuseong-gu, Daejeon 34141, Republic of Korea
[*]Corresponding author:yongheekim@kaist.ac.kr

1. Introduction

The deterministic truncation of Monte Carlo (DTMC) solution is a deterministic solution truncated from the original MC calculation assisted by coarse mesh finite difference (CMFD) method [1-2]. This idea was proposed as a variance reduction technique applied in the MC simulation. In the conventional CMFD method, the results are only used to update the fission source distribution (FSD). However, in the DTMC method, the deterministic results are used not only to update the FSD, but also to provide the detailed reactor information by itself with a pin-size CMFD node. Since the DTMC solution is estimated in a deterministic way and minimizes the uncertainties coming from the MC random process, it may be able to provide quite reliable solutions from early active cycles.

The CMFD and DTMC solutions can be improved with the optimization of the boundary condition. Since the correction factors at boundary regions are defined by the simple ratio of the neutron current and flux, its accuracy and reliability highly depend on the CMFD parameters. However, the CMFD parameters are more uncertain near the boundary regions due to low neutron density. This can make the DTMC solutions less reliable. Therefore, this paper proposes a way of particle splitting method with the weight window scheme to improve and optimize the albedo boundary condition in the DTMC method. This is expected to enhance reliability of CMFD parameters near the boundary and improve the DTMC solutions.

2. Methods and Results

In this section the concept of the DTMC is introduced and the boundary condition in the DTMC method is presented to understand the importance of the albedo boundary condition. The theory of the particle splitting with the weight window method is presented.

2.1 DTMC method

The DTMC is the deterministic solution truncated in a systematic way from the MC solution assisted by the CMFD method. The CMFD parameters such as the neutron current, flux, and cross-section are calculated from the MC simulation, the correction factors are generated with the parameters, and the matrix equation is formulated. By solving the matrix equation of the reactor eigenvalue problem, the reactor parameters such as the multiplication factor and the detailed power distribution are obtained. The results are used not only to update the FSD of the subsequent MC calculation by correcting the particles' weight, but also used for statistical samples to predict the solution by themselves. (Fig. 1) [3]
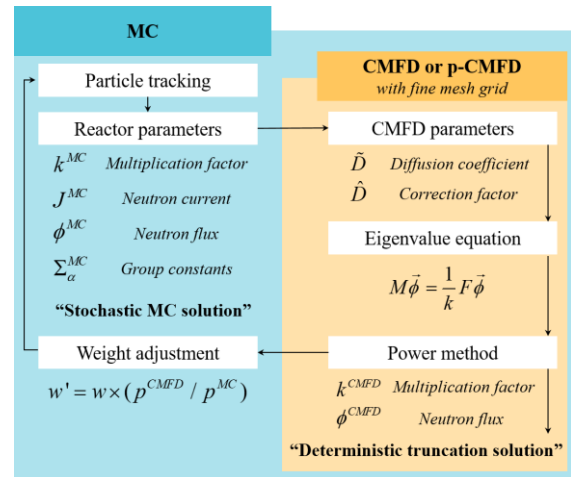
Fig. 1. Flow diagram of CMFD and DTMC

The DTMC method basically adopts the fine mesh grid to calculate the detailed pin-wise power profile as well as the multiplication factor. The DTMC method highly depends on the CMFD parameters estimated from the MC simulation, but it can be rather insensitive to the stochastic random process of the MC simulation because it is calculated by the deterministic way. Therefore, it minimizes the uncertainties of the solution and reduce the computational burden.

2.2 Boundary region and condition

To get the reliable CMFD parameters, many histories of the neutrons should be stored in the CMFD node. Therefore, the domain for the CMFD calculation is normally confined to an active core region where the neutrons are born and thus the neutron density is high. The non-fissionable region like a reflector is excluded. It can decrease the uncertainty of the node-wise parameter and also cut down the numerical cost by reducing the number of calculation nodes.

In the CMFD method, the correction factor within the boundary is calculated with the net current and the neighboring fluxes.

$$\hat{D}^{s+1/2} = \frac{\vec{J}^{s+1/2} + \tilde{D}^{s+1/2}(\phi^{i+1} - \phi^{i})}{\phi^{i+1} + \phi^{i}} \quad (1)$$

where $\vec{J}^{s+1/2}$ is the net current, ϕ^{i} is the neutron flux at node i, $\tilde{D}^{s+1/2}$ is the effective diffusion coefficient defined by

$$\tilde{D}^{s+1/2} = \frac{2(D^{i+1}/\Delta^{i+1})(D^{i}/\Delta^{i})}{(D^{i+1}/\Delta^{i+1}) + (D^{i}/\Delta^{i})}$$

D^{i} is the diffusion coefficient at node i, Δ^{i} is the node size, and s is the surface index. On the other hand, the correction factor at the boundary surface is calculated by the ratio of net current and flux.

$$\hat{D}^{s+1/2} = \vec{J}^{s+1/2}/\phi^{i} \quad (2)$$

The two terms in the numerator of Eq. (1) are similar each other and cancelled out. In short, the correction factor of Eq. (1) gets less sensitive to the CMFD parameters. Comparing to the correction factor within the boundary, the correction factor at the boundary surface is more related to the CMFD parameters i.e. current and flux. Its accuracy highly depends on the parameters. Besides, the CMFD parameters are more unreliable near the boundary region due to low neutron density. Therefore, the correction can be inaccurate near the boundary and it will influence on final solutions.
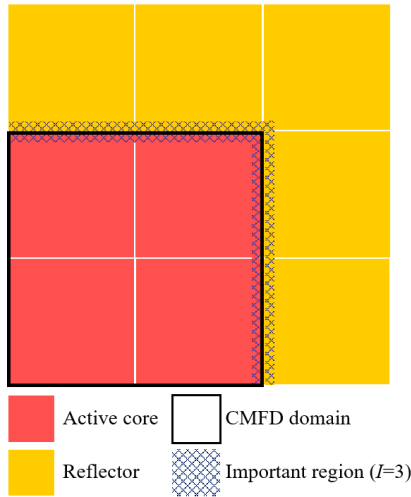
Fig. 2. CMFD Domain and important region

To increase the number of histories and reliability of the CMFD parameters at the boundary region, the neutron are split into many neutrons with the low weight by the weight window method. In the important region, the more number of particles can be simulated while preserving the net weight of the particles.

In Fig. 2, the boundary layer and the region of importance are illustrated. The CMFD domain is confined to the active core, and the higher importance is assigned to the cells surrounding the boundary layer. In

this way, it increase the histories exclusively at the boundary region.

2.3 Particle splitting with weight window method

For the parameter to be reliable, many histories should be recorded in the given space. However, it is impractical to use many histories per cycle in the MC simulation. It is computationally expensive and inefficient. Therefore, it is pursued to simulate the more number of particles at the specific regions of interest.

In the particle splitting with weight window method, the single particle can be divided into many particles at the important region without the numerical bias [4]. The weight of the particle should be decreased as the more neutrons are split. In short, the total net weight of the particles should be preserved.

Suppose that the neutron is crossing the surface from the low importance region to the high importance region. Then the neutron is divided into many neutrons according to the ratio of importance. The number of split neutrons is

$$n = I_{i+1}/I_{i} \quad (3)$$

and the weight of each neutron is

$$w_{i+1} = w_{i}/n \quad (4)$$

where the ratio of importance is integer.
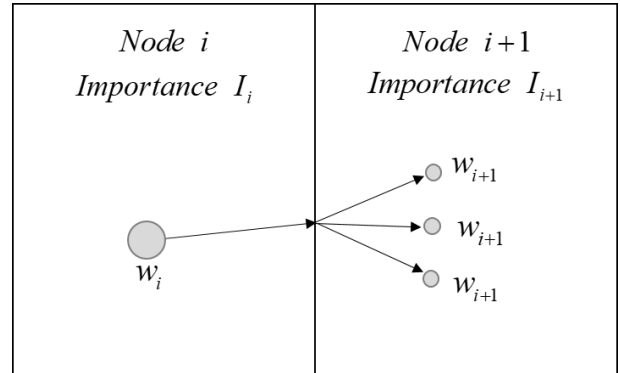
Fig. 3. Particle crossing to different importance region

On the other hand, if the neutron passes from the high importance region to the low importance region, it is tracked with higher weight or killed based on the probability such that

$$kill \ with \ 1 - p = 1 - I_{i+1}/I_{i}$$

$$live \ with \ p = I_{i+1}/I_{i} \ and \ w_{i} = w_{i+1} \cdot I_{i+1}/I_{i}$$

In this analysis, the cell importance in the boundary area is 3 while the importance in the other area is 1. The higher importance is assigned to the last fuel pin and the neighboring reflector pin in the radial direction, and from 14.27 cm of upper core to 7.14 cm of reflector in the axial direction.

2.4 Problem description

Benchmark problem was solved to verify the numerical performance of the albedo boundary correction in the DTMC method. A multi-group in-house MC code has been used for the MC and DTMC calculations. The 3D rodded A-type C5G7 benchmark was solved with the dominance ratio of 0.978. The quarter core is considered with UO_2 and MOX fuel assemblies arranged in a checkerboard pattern surrounded by the reflector. The control rods are inserted to the one-third of the way into the center UO_2 assembly. (Figs. 4 and 5) [5]
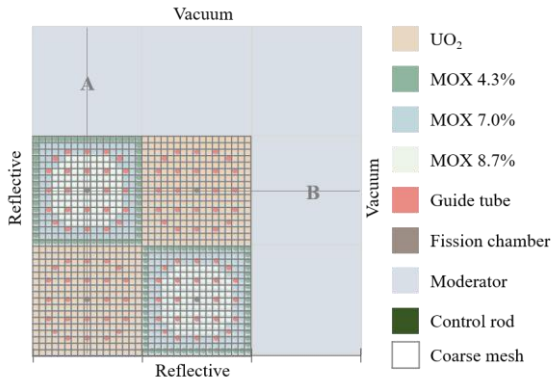
Fig. 4. Radial configuration of C5G7 core
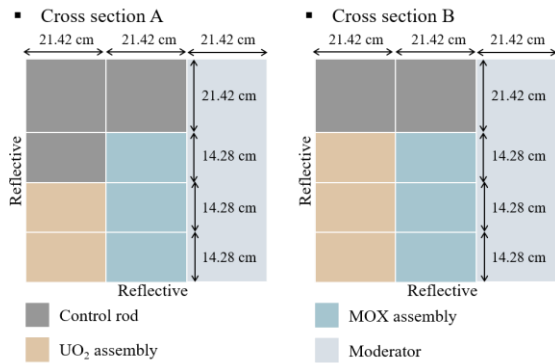
Fig. 5. Axial configuration of C5G7 core

The million histories per cycle and 100 active cycles were adopted for the MC simulation. Sixty independent simulations were implemented to calculate the real standard deviation. The CMFD node was taken to be single pin size (1.26×1.26 cm^2) in the radial direction and 14.28 cm in the axial direction.

2.5 Numerical results

Table I summarizes the multiplication factors and their stochastic uncertainties such as the apparent standard deviation (σ_a) and real standard deviation (σ_r), and compares the results between the methods including the standard MC (MC), MC results assisted by CMFD method (CMFD), and DTMC method (DTMC) with the different importance. The real standard deviation is calculated as

$$\sigma_r = \frac{1}{N_b} \sum_{i=1}^{N_b} (k_{eff}^i - \bar{k})^2$$

where N_b is the number of batches, k_{eff}^i is the multiplication factor of batch i, and $\bar{k}$ is the average of batch-wise k_{eff}.

Table I. Multiplication factors and their stochastic uncertainties at certain cycles

Importance			1		3	
Cycle	Variable	MC	CMFD	DTMC	CMFD	DTMC
1	k_{eff}	1.12867	1.12845	1.12821	1.12734	1.12801
	σ_a (pcm)	64.2	68.5	29.3	69.6	30.5
	σ_r (pcm)	85.7	83.3	43.1	83.7	43.8
5	k_{eff}	1.12783	1.12834	1.12826	1.12817	1.12802
	σ_a (pcm)	39.2	39.9	22.1	43.3	21.9
	σ_r (pcm)	53.0	53.6	29.5	45.1	23.8
10	k_{eff}	1.12787	1.12826	1.12842	1.12811	1.12784
	σ_a (pcm)	30.2	31.3	17.1	33.0	17.0
	σ_r (pcm)	40.1	37.8	23.0	33.0	16.2
20	k_{eff}	1.12810	1.12807	1.12824	1.12792	1.12788
	σ_a (pcm)	21.9	23.3	12.4	24.8	12.6
	σ_r (pcm)	25.7	27.7	16.9	26.2	13.5
100	k_{eff}	1.12819	1.12811	1.12818	1.12790	1.12796
	σ_a (pcm)	10.2	11.0	5.9	11.3	5.7
	σ_r (pcm)	12.2	12.7	7.0	11.8	6.9
	σ_r/σ_a	1.20	1.15	1.19	1.04	1.21
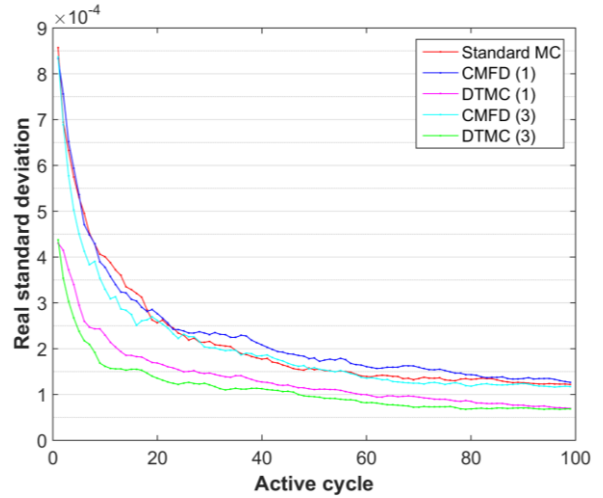
Fig. 6. Real standard deviation of k_{eff}

The results with the particle splitting method show smaller statistical uncertainties compared to the standard MC and conventional CMFD and DTMC methods. Fig. 6 shows the real standard deviation of the multiplication factor along with the cycle. The σ_r of the DTMC with the particle splitting method is slightly lower than that of other methods.

Table II summarizes the average real standard deviation ($\bar{\sigma}_r$) and average errors ($\bar{\varepsilon}$) of 3D pin-wise power profile at the certain cycles, Table III compares the errors of 2D assembly wise power profile, and Fig. 7 shows the average relative errors (%) of the power distribution of the 3rd layer. One can note that the particle splitting method also reduces the standard

deviation (SD) and errors in terms of the pin power distribution particularly in the boundary region. It is clearly observed that peak error in the 3D power profile is noticeably reduced.

Table II. SD and errors of 3D pin power profile

Importance		1			3	
Cycle	Variable	MC	CMFD	DTMC	CMFD	DTMC
1	$\bar{\sigma}_r$ (pcm)	0.038	0.038	0.034	0.034	0.030
	ε_{max} (%)	**10.50**	**10.30**	**9.23**	**7.53**	**6.75**
	ε_{avg} (%)	0.57	0.58	0.51	0.53	0.47
5	$\bar{\sigma}_r$ (pcm)	0.022	0.022	0.021	0.020	0.019
	ε_{max} (%)	**5.56**	**5.89**	**5.39**	**3.74**	**3.55**
	ε_{avg} (%)	0.37	0.37	0.35	0.34	0.33
10	$\bar{\sigma}_r$ (pcm)	0.016	0.016	0.016	0.015	0.014
	ε_{max} (%)	**4.03**	**4.28**	**4.18**	**2.90**	**2.88**
	ε_{avg} (%)	0.27	0.27	0.27	0.25	0.25
20	$\bar{\sigma}_r$ (pcm)	0.012	0.012	0.012	0.011	0.010
	ε_{max} (%)	**3.02**	**3.19**	**3.29**	**2.07**	**2.04**
	ε_{avg} (%)	0.20	0.20	0.19	0.18	0.18
100	$\bar{\sigma}_a$ (pcm)	0.005	0.005	0.004	0.005	0.004
	$\bar{\sigma}_r$ (pcm)	0.005	0.005	0.005	0.005	0.005
	ε_{max} (%)	**1.422**	**1.445**	**1.433**	**1.414**	**1.382**
	ε_{avg} (%)	0.093	0.092	0.091	0.086	0.085

Table III. SD and errors of 2D assembly power profile

Importance		1			3	
Cycle	Variable	MC	CMFD	DTMC	CMFD	DTMC
1	ε_{avg} (%)	0.233	0.308	0.305	0.302	0.330
	ε_{max} (%)	0.336	0.398	0.406	0.425	0.428
5	ε_{avg} (%)	0.188	0.219	0.199	0.187	0.186
	ε_{max} (%)	0.239	0.322	0.304	0.248	0.236
10	ε_{avg} (%)	0.160	0.150	0.137	0.146	0.141
	ε_{max} (%)	0.211	0.218	0.194	0.215	0.203
100	ε_{avg} (%)	0.077	0.065	0.061	0.072	0.068
	ε_{max} (%)	0.101	0.081	0.075	0.102	0.095

Computing time for each method was compared in Table IV. The computing time increases with the particle splitting method because more number of particles should be simulated in the higher-importance regions. If the active core includes the high importance region, time increase can be quite noticeable because fission neutrons should be also split and then the number of neutrons in a higher importance region can increase substantially.

The current model includes higher importance regions in the active core, which is 14.28 cm of the upper core. It considerably increases the computing time. To decrease the computing time, the axial size should be minimized. However, if the node is too small, the node-wise parameters can be less reliable. Therefore, the optimal node size should be found to minimize the additional computing time while improving the accuracy of the solutions.
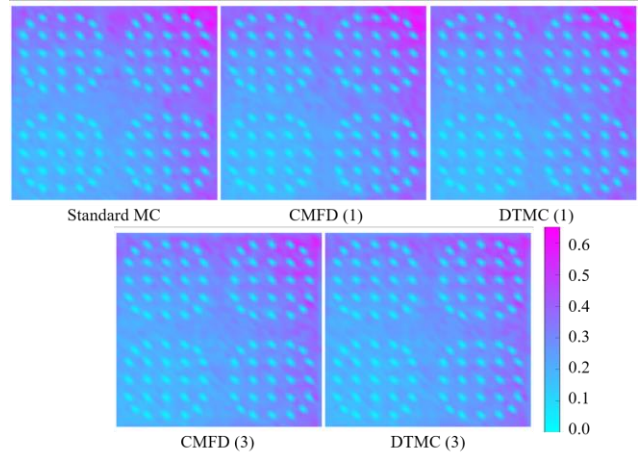
Fig. 7. Relative errors of power distribution at 3rd layer

Table IV. Computing time of the simulation

Parameter	Time (min)
MC	45
CMFD / DTMC (1)	46
CMFD / DTMC (3)	62

3. Conclusions

The CMFD and DTMC solution was improved with the optimization of the albedo boundary condition. The statistical uncertainties were decreased and the errors of the pin-wise power distribution were decreased particularly near the boundary region. However, the computing time also increased noticeably because the number of particles to be simulated increased substantially in the fuel region. Therefore, the area and position of the important region should be optimized to decrease the computing time while improving the accuracy of the boundary conditions.

REFERENCES

[1] Inhyung Kim and Yonghee Kim, A Study on CMFD Trucation of Monte Carlo Neutron Transport Solution, *Transactions of the Korean Nuclear Society Autumn Meeting*, Gyeongju, Korea, October 25-27, 2017
[2] Inhyung Kim and Yonghee Kim, A Study on Deterministic Truncation of Monte Carlo Transport Solution, *PHYSOR 2018*, Cancun, Mexico, April 22-26, 2018
[3] Inhyung Kim and Yonghee Kim, A Comparative Study on CMFD and p-CMFD Acceleration in the Monte Carlo Analysis, *Proceedings of the American Nuclear Society* (ANS), Washington, DC, USA, 2017
[4] Booth T. E. and Hendricks J. S. Importance estimation in Forward Monte Carlo Calculation, *Nuclear Technology /Fusion*, **5**, 1984
[5] OECD/NEA. "Benchmark on Deterministic Transport Calculations without Spatial Homogenisation," Organization for Economic Cooperation and Development, (2005)